Morphology–Toughness Correlation of Polypropylene/Ethylene–Propylene Rubber Blends

Ines Kotter,[1] Wolfgang Grellmann,[1] Thomas Koch,[2] Sabine Seidler[2]

[1]*Department of Engineering Science, Institute of Materials Science, Martin-Luther-University Halle-Wittenberg, D-06099 Halle (Saale), Germany*
[2]*Institute of Materials Science and Technology, Vienna University of Technology, A-1040 Vienna, Austria*

Received 26 July 2004; accepted 2 November 2005
DOI 10.1002/app.23708
Published online in Wiley InterScience (www.interscience.wiley.com).

ABSTRACT: A polypropylene homopolymer was blended with ethylene–propylene rubber in different mixing ratios. The influence of the ethylene–propylene rubber content on the toughness behavior was investigated. According to the results of instrumented impact tests, brittle-to-tough transition temperatures were found for different ethylene–propylene rubber contents. Critical transition temperatures could be determined not only in the region of predominantly unstable crack propagation but also in the region of stable crack initiation. In situ measurements provided information on the deformation processes on the crack tip. © 2006 Wiley Periodicals, Inc. J Appl Polym Sci 100: 3364–3371, 2006

Key words: fracture; poly(propylene) (PP); toughness; brittle-to-tough transition temperatures; in situ investigations; crack resistance curve

INTRODUCTION

Polypropylene (PP) is a semicrystalline, thermoplastic polymer with a wide range of applications (e.g., in the packaging and food industries, in the automotive industry, and in electrical appliances).

The wide field of applications is restricted because of the low toughness at temperatures below the glass-transition temperature (T_g; T_g for PP $\approx$ 0°C). The incorporation of an elastomeric phase enhances the toughness at temperatures below 0°C also.

The mechanical properties of such toughened heterophasic polymers depend on the type and volume content of the elastomeric phase and on the interactions between the two phases. Toughened PP is applied, for example, as a bumper material in the automotive industry. In this case, a high energy absorption capacity is significant under impact conditions and at low temperatures too.

To exploit the capacity of the materials, knowledge of the correlation between the morphology and mechanical properties, particularly the toughness behavior, is required. The toughness, that is, the resistance against stable and unstable crack propagation, is described by fracture mechanical values. These values can reflect changes in morphological parameters, such as the modifier content, size, and interparticle distance. Wu[1] determined a critical interparticle distance for blends with spherical elastomeric particles. If the interparticle distance is below this critical value, the toughness increases rapidly because of the shear yielding of the matrix between the particles. The author defined the critical interparticle distance for a specified testing temperature and testing velocity as a constant of the matrix material, independent of the modifier content and particle diameter. This constant can be determined for all polymer rubber blends with matrix–particle morphology, for which toughening occurs with increasing shear-yielding processes. Starke et al.[2] found a linear dependence of the critical interparticle distance on the temperature for a heterophasic reactor-grade propylene–ethylene copolymer. Borggreve et al.[3] and Margolina[4] determined this dependence for rubber-modified nylons.

Mamath et al.[5] detected a change in the morphology from matrix–particle to cocontinuous by increasing the modifier content for polyamide 6/acrylonitrile-butadiene-styrene (ABS) blends. The stiffness decreased linearly and the toughness increased rapidly during morphology changes with increasing ABS content. The authors found a critical modifier content at which the transition from brittle material behavior to tough material behavior occurred.

As a rule, the brittle-to-tough transition is described with the conventional notched impact strength. With this value, the crack-growth process cannot be separated into a stable part and an unstable part. Two critical interparticle distances were determined by Grellmann et al.[6] for heterophasic propylene–ethylene copolymers using fracture mechanics values. At first, a

Correspondence to: W. Grellmann (wolfgang.grellmann@iw.uni-halle.de).

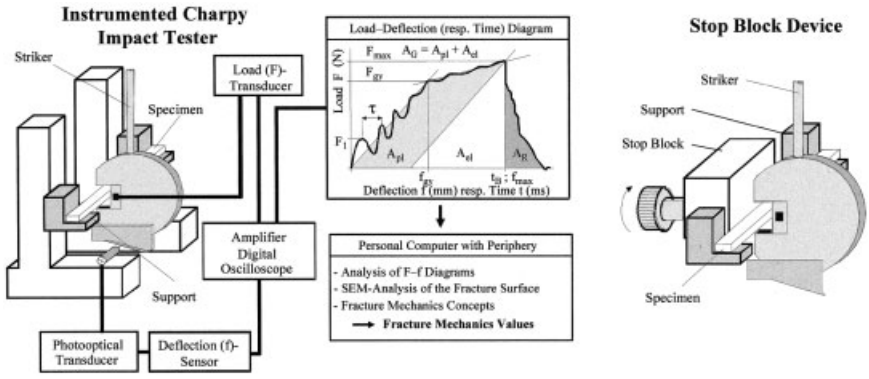

Figure 1 Fracture mechanics testing device for the instrumented Charpy impact tests.

transition from brittle material behavior to tough material behavior takes place. Furthermore, a transition from tough material behavior to high-impact material behavior has been found.

In this article, fracture mechanics tests are described for stable and unstable crack propagation under impact and quasi-static loading conditions. Energy-dissipation processes in front of the crack tip characterize the toughness behavior. These processes have been observed with scanning electron microscopy (SEM).

EXPERIMENTAL

Material

Blends containing isotactic PP and ethylene–propylene rubber (EPR) were used. The noncrosslinked EPR was a commercial master batch that consisted of 65 wt % amorphous EPR and 35 wt % semicrystalline polyethylene (PE). The PE inclusions in the EPR phase reduced the loss of material stiffness and improved the toughness behavior because of the increase in the energy dissipation of modified microdeformation processes.

To determine the influence of the elastomeric phase on PP materials over a wide range, the blends were produced in a twin-screw extruder in a mixing series from 100 wt % PP up to 15 wt % PP and 85 wt % EPR. According to the standard ISO 179-2,[7] single-edge-notched bending (SENB) specimens were used. The dimensions of the injection-molded specimens were 80 mm × 10 mm × 4 mm.

Fracture mechanics characterization

To determine the toughness behavior under impact loading, an instrumented Charpy impact tester with a 4-J work capacity was used, and load–deflection diagrams were registered. The load was recorded by strain gauges positioned directly on the striker edge; the deflection was measured by a photooptical transducer. The detailed procedure for determining the crack-resistance behavior with the instrumented Charpy impact test is described elsewhere.[8,9] The testing device is drafted in Figure 1.

The SENB specimens were notched with a razor blade (notch tip radius = 0.2 μm). The support span was 40 mm (support span/width = 4); the pendulum hammer speed was 1.5 ms^{-1}. To determine the fracture mechanics values as the resistance against unstable crack propagation, the initial crack length was 2 mm (initial crack length/width = 0.2). Concepts of elastic–plastic fracture mechanics, such as the COD and *J*-integral concepts, were applied. The COD concept is based on the assumption that the fracture process is controlled by plastic deformation in front of the crack tip. The COD value is the critical crack opening displacement (δ_d), the deformation-determined loading parameter.

The energy determined *J*-integral values (J_{id}^{ST}) were based on the approximation of Sumpter and Turner,[10] which splits the specimen deformation energy (A_G) into an elastic part (A_{el}) and a plastic part (A_{pl}).

If the crack growth was predominantly stable, the crack-resistance-curve concept was used to determine the fracture mechanical values as resistance against stable crack initiation and propagation.

There, the initial crack length was 4.5 mm (initial crack length/width = 0.45), and the multiple-specimen method was used.

We generated different lengths of stable crack growth (Δa) by enabling different defined deflections using the stop block device (Fig. 1). A crack-resistance curve is the relation between a loading parameter [e.g., the crack opening displacement (δ) as a deformation-determined parameter or *J* as an energy-determined parameter] and Δa.

The technical crack-initiation values $\delta_d^{0.2}$ and $J_d^{0.2}$ were determined at Δa = 0.2 mm. The resistance against stable crack growth is described by the tearing modul $T_{\delta d}^{0.2}$ and $T_J^{0.2}$. These values were calculated with the slope of the crack-resistance curve in conjunc-

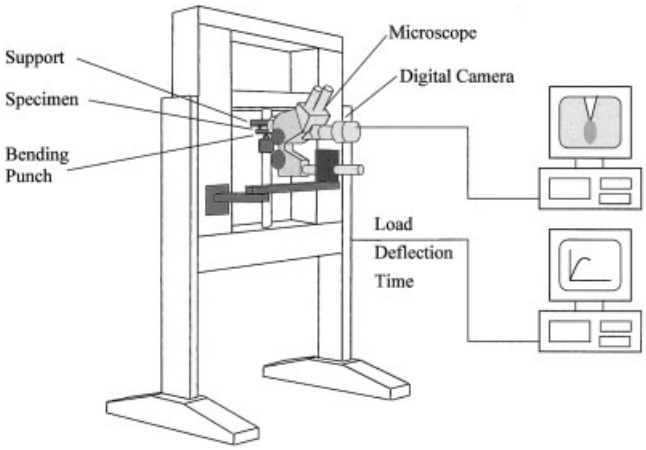

Figure 2 Testing device for the in situ determination of the crack-resistance behavior at a quasi-static loading.

tion with the dynamic flexural modulus and dynamic yield stress.[8]

With J–T_J stability assessment diagrams, values could be determined as the resistance against unstable crack propagation for materials that showed no unstable failure under the given experimental test conditions.[8,11] With such diagrams, there was the possibility of determining instability values over a wide range of temperatures and compositions, independently of the crack-growth process, as shown in ref. 2.

In situ investigations were performed to observe and quantify the crack-initiation process. Furthermore, crack-resistance curves under quasi-static loading conditions could be determined with only one specimen. The SENB specimens (initial crack length/width = 0.2) were side-grooved to get a planar crack front. The in situ investigations were carried out on a universal testing machine with a three-point-bending device. The crosshead speed was 10 mm/min. The experimental setup is shown in Figure 2. An optical microscope coupled with a digital camera was located in front of the crack tip. Pictures of the specimen surface could be saved during the loading process. The testing time, load, and deflection were recorded. δ and Δa were directly measured at the surface of the specimen. δ plotted as a function of Δa described the crack-resistance behavior (δ_R curve). This curve was measured in situ with only one specimen (single-specimen method). The J-integral values were calculated with the recorded load–deflection curves. These curves were validated by the recording of five tests for each investigated material.

Microdeformation processes in front of the crack tip control the toughness behavior of the material. To investigate these processes, SENB specimens were defined loaded. The opened crack tips were fixed with an epoxy resin; the centers of the crack-tip areas were cryomicrotomed, gold-sputtered, and observed by SEM.

Furthermore, the investigated materials were characterized as follows:

- Transmission electron microscopy (TEM) was used to analyze the morphology of the materials. The microtomed, ultrathin slices were stained with ruthenium tetroxide (RuO_4).
- Dynamic mechanical analysis (DMA) was used, with a torsional device with a frequency of 1 Hz and a heating rate of 2 K/min, to determine T_g of the amorphous phases of PP and EPR.
- Differential scanning calorimetry (DSC) was used, with the Mettler–Toledo DSC 820 instrument (Greifensee, Switzerland), to detect the melting temperatures and the crystallinities at 10 K/min.
- Quasi-static tensile tests were used in accordance with the standard ISO 527[12] at different temperatures to determine the mechanical behavior at a uniaxial loading.
- Further mechanical tests were used to determine the flexural modulus (E_f) and the notched Charpy impact strength (a_{cN}) of the material.

RESULTS AND DISCUSSION

Morphology

TEM investigations show a matrix–particle morphology up to 30 wt % EPR [Fig. 3(a)]. Then, a transition to a cocontinuous morphology can be observed [Fig. (3b,c)]. At a mixing ratio of 15 wt % PP and 85 wt % EPR, a phase change occurs; EPR is the matrix material, and the PP phase is dispersed [Fig. 3(d)]. The EPR phase of the blends shows a heterogeneous structure. The amorphous EPR of the master batch appears darker because of the staining agent. Within the EPR, semicrystalline PE inclusions are evident. Therefore,

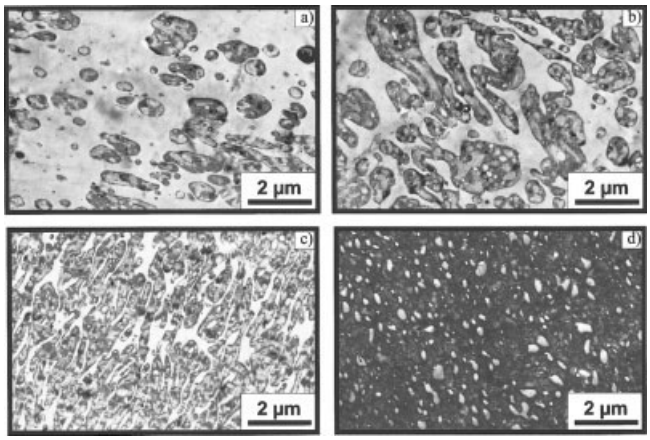

Figure 3 TEM micrographs of PP/EPR blends with several mixing ratios: (a) 70 wt % PP/30 wt % EPR, (b) 50 wt % PP/50 wt % EPR, (c) 30 wt % PP/70 wt % EPR, and (d) 15 wt % PP/85 wt % EPR.

TABLE I
Basic Characterization of the PP/EPR Blends and Their Mechanical and Thermal Parameters

PP/EPR mixing ratio (wt %)	DMA		DSC		Bending test		
	EPR T_g (°C)	PP T_g (°C)	PP T_m (°C)	H_m (J/g)	E_f (MPa)	σ_{fc} (MPa)	a_{cN} at 23°C (kJ/m^2)
100/0	—	17.2	164	109.2	1299	32.5	3.0
85/15	−56.1	17.8	164	68.2	1028	26.8	7.9
70/30	−54.5	17.0	162	54.5	810	20.6	44.6
60/40	−53.7	18.5	162	46.6	656	16.3	64.5
50/50	−52.6	18.8	161	38.5	487	11.9	67.6
40/60	−51.8	17.7	163	30.6	364	8.7	65.3
30/70	−50.2	18.4	164	20.9	248	5.8	55.2
15/85	−50.8	—	162	15.2	100	2.6	9.2

the amorphous EPR is the adhesive layer between PP and EPR. The mixing series contains the following:

- Pure PP.
- Matrix–particle morphology (PP matrix and EPR particles).
- Cocontinuous morphology.
- Matrix–particle morphology (EPR matrix and PP particles).

Therefore, the correlations between the morphology and toughness behavior can be discussed only with respect to the EPR content.

Basic characterization

Information on the mechanical and thermal behavior of the blends is given in Table I.

If the components of multiphase polymeric systems are immiscible, the α-relaxation areas of the components are separated in DMA investigations. From the course of the mechanical loss factor, T_g can be determined. Although T_g of the PP phase is constant for all blends, T_g of the EPR phase shifts to higher temperatures with increasing EPR content. Residual tensile stress occurs during blending in the EPR phase. These stresses lead to an increase in the free volume, so the mobility of the molecules increases.

The melting temperature of PP is nearly independent of the EPR content. The heat of fusion increases with increasing PP content, but the degree of crystallinity is unaffected and constant.

For the description of the mechanical behavior at room temperature, E_f and the standard flexural strength (σ_{fc}) according to ISO 178[13] and a_{cN} in accordance with ISO 179-1[14] are used. E_f and σ_{fc} decrease with increasing EPR content, in contrast to a_{cN}, which exhibits an optimum at 50 wt % EPR. The mechanical material behavior of elastomerically modified PP depends on morphological parameters as well as loading conditions, that is, the testing temperature or testing velocity. At testing temperatures below T_g's of both components, the blends show brittle stress–strain behavior. The mobility of the molecules is very low, and the alignment is rigid, so nearly no relaxation processes and sliding mechanisms of the molecule chains occur. The molecule mobility increases with temperature, so the modulus of elasticity (E_t; Fig. 4) and the tensile strength decrease. Furthermore, molecule sliding increases with increasing temperature. It leads to higher ductility of the material characterized by strain at break (ε_B; Fig. 4).

Crack-resistance behavior under impact loading

At low testing temperatures and/or low EPR contents, the material behavior is linear–elastic. The crack grows in an unstable manner. In a small transfer region, elastic–plastic behavior connected with unstable crack propagation can be observed. At higher EPR contents and/or higher temperatures, stable crack growth with incomplete fracture of the specimen takes place.

The critical J values are determined with the energy that is dissipated during the fracture process. This means that the temperature dependence of the J values is stamped by the temperature dependence of both

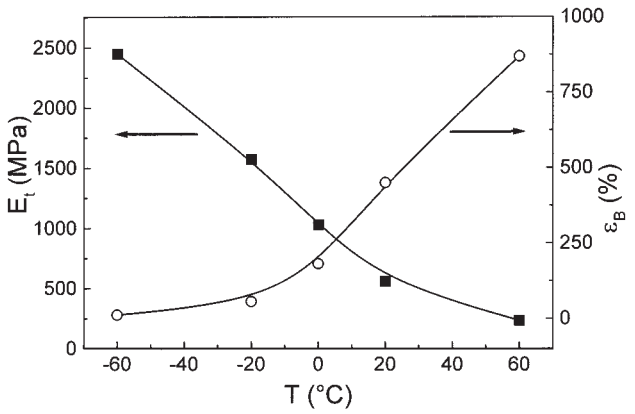

Figure 4 E_t and ε_B versus the testing temperature (T).

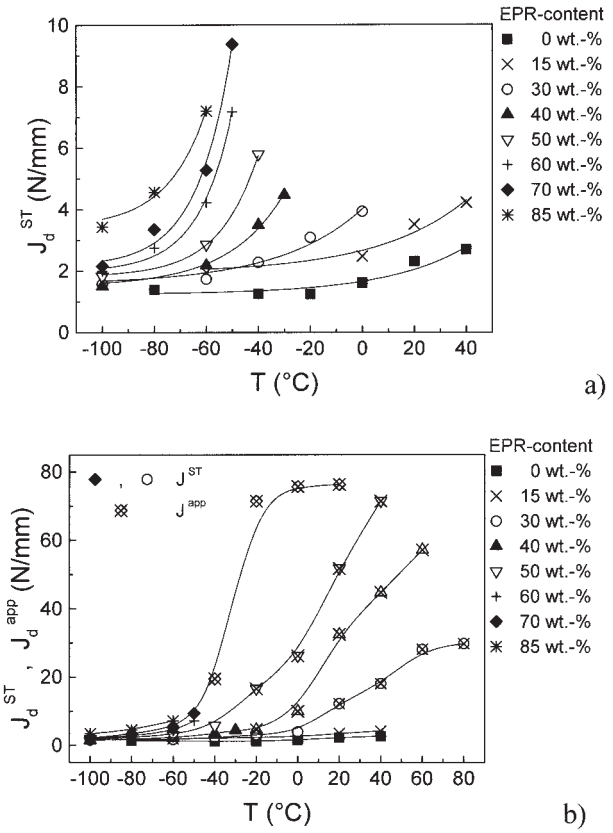

Figure 5 Critical J values of PP/EPR blends with different EPR contents versus the testing temperature (T): (a) experimental (J_d^{ST}) and (b) J_d^{ST} and approximated (J_d^{app}) values.

the maximum load and maximum deflection. Figure 5(a) shows the dependence of experimentally determined critical J values on the testing temperature and the EPR content. At −100°C, the J values are independent of the EPR content at low levels, with the exception of the blend with 85 wt % EPR (EPR matrix). For this, the resistance against unstable crack propagation is well above the values of the other materials. The matrix material PP shows at testing temperatures below 0°C athermic fracture behavior. The transition of the low level to higher J values shifts with increasing EPR content to lower testing temperatures. The transition from dominant unstable crack propagation to dominant stable crack growth shifts in a similar manner.

The experimental method for determining instability values with J–T_J stability assessment diagrams is especially applicable to PP/EPR blends.[8] The experimental J values in Figure 5(b) are completed by approximated values. With increasing temperature, the rise of the approximated values for the blend with matrix–particle morphology is much lower than the rise of the blends with cocontinuous morphology. Without comprehension of the approximated values, a complete description of the toughness behavior as resistance against unstable crack propagation with respect to the mixing ratio as well as temperature is not possible.

For fracture mechanics characterization of the deformation behavior, the COD concept was applied, and δ_d was determined. The δ_d values (Fig. 6) show a dependence on the EPR content and temperature similar to that of the J values. This means that the crack-resistance behavior of the blends is mainly determined by deformation processes.

To exploit the material properties more effectively, the resistance against stable crack initiation and propagation was determined by the application of the crack-resistance-curve concept. The curve progressions of the blends with cocontinuous morphology are identical at a testing temperature near T_g of the elastomeric phase [Fig. 7(a)].

At this low temperature, a significant rise in the toughness can be reached only by a change in the phase morphology. At testing temperatures between T_g's of both phases, the curve progression is more influenced by the EPR content than by the morphology [Fig. 7(b)].

As shown in Figure 8(a), at −20°C, the crack-initiation value gradually increases up to 70 wt % EPR and rapidly thereafter. In contrast, at −20°C, $T_{\delta d}^{0.2}$ increases linearly with increasing EPR content, regardless of the phase morphology [Fig. 8(b)]. That means in a temperature range between the T_g's of both phases, a rise in the EPR content affects the crack propagation more than the crack initiation. At −40°C, a rise in critical toughness values can be observed after phase changes only. At testing temperatures below T_g of the EPR phase, no significant rise in the toughness values occurs.

Determination of the transition temperatures in the case of stable crack initiation and unstable crack propagation

In Figures 5(a) and 6, toughness values as the resistance against unstable crack propagation are shown as

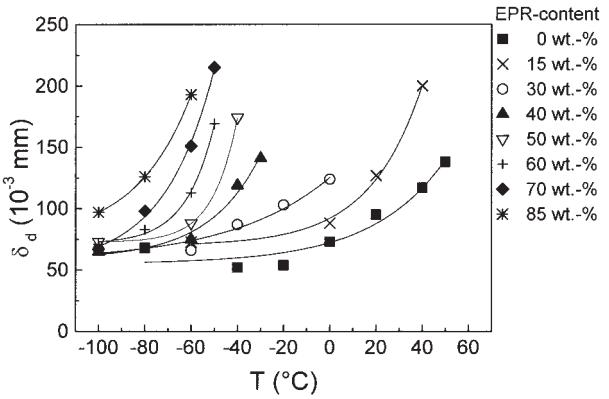

Figure 6 Critical experimental δ_d values of PP/EPR blends with different EPR contents versus the testing temperature (T).

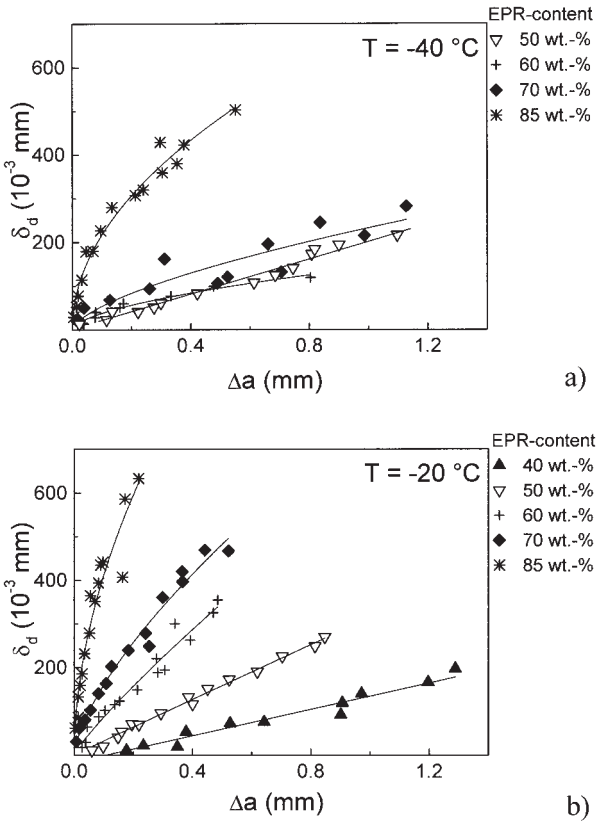

Figure 7 Crack-resistance curves for blends with higher EPR contents: (a) testing temperature (T) = −40°C and (b) T = −20°C.

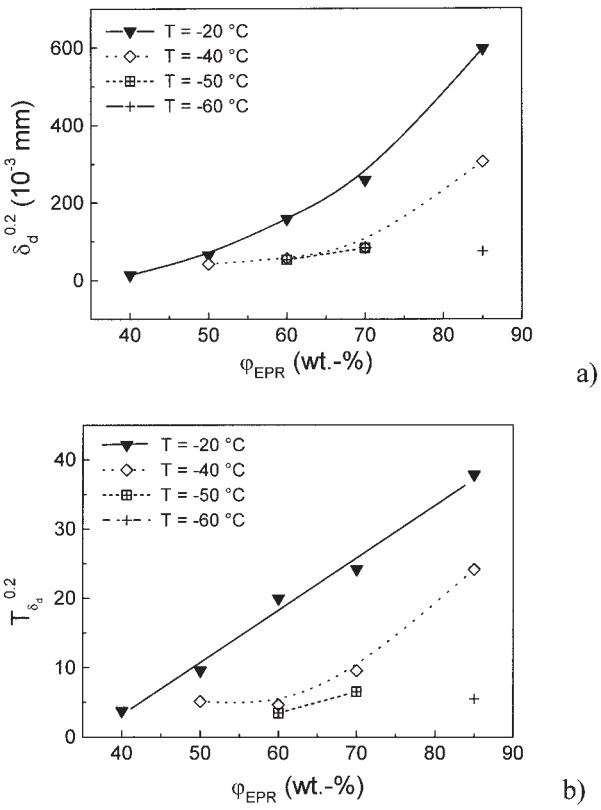

Figure 8 Fracture mechanics values versus the EPR content (ϕ_{EPR}) for several temperatures (T): (a) $\delta_d^{0.2}$ and (b) $T_{\delta d}^{0.2}$.

a function of temperature. From these plots, we can see that each blend has a certain transition temperature. Above this temperature, the toughness values increase rapidly.

Such transition temperatures can be determined at the point of intersection of two tangents applied to the toughness–temperature curve (Fig. 9). The transition temperature in the region of unstable crack propagation is defined as the brittle-to-tough transition temperature (T_{BTT}). In the region of stable crack initiation, a tough-to-high-impact transition temperature (T_{THT}) is established.

For several blends of the mixing series, both transition temperatures were determined according to Figure 9 with the experimental toughness values. The transition temperatures are shown for blends with different EPR contents in Figure 10.

In contrast to toughened amorphous polymers,[15] both transitions show an exponential decrease as the EPR content decreases; that is, the lower the temperature is, the higher the EPR content must be to get sufficient toughness. The diagram in Figure 10 can be used for the determination of application-oriented temperatures and limitations.

Crack-resistance behavior under quasi-static loading

In situ investigations of pure PP and blends with lower EPR contents have enabled the determination of the crack-initiation point at the load–deflection curve above the linear–elastic part but below the maximum load.[16] The specimen of pure PP failed in an unstable manner when the maximum load was reached. The blends reached the maximum deflection without specimen failure.

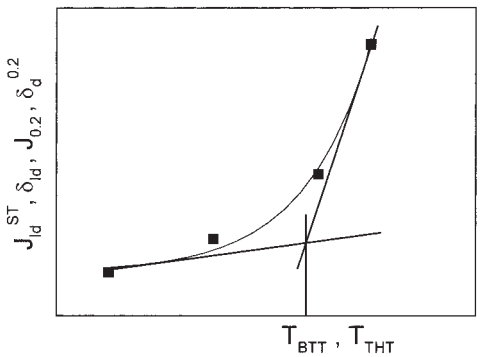

Figure 9 Schematic diagram for the determination of the transition temperatures with the temperature dependence of the toughness values.

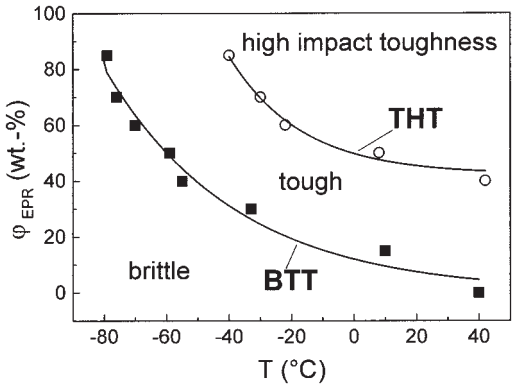

Figure 10 Brittle-to-tough transition (BTT) temperatures and tough-to-high-impact-toughness transition (THT) temperatures versus the EPR content (ϕ_{EPR}).

Representative single-specimen crack-resistance curves are shown in Figure 11. The blends containing 30 and 40 wt % EPR show only a very small difference, although the morphology differs significantly. At this low testing speed, the process of relaxation appearing during loading is independent of the blend composition and phase morphology when a critical EPR content is exceeded. The critical EPR content can be found between 15 and 30 wt %.

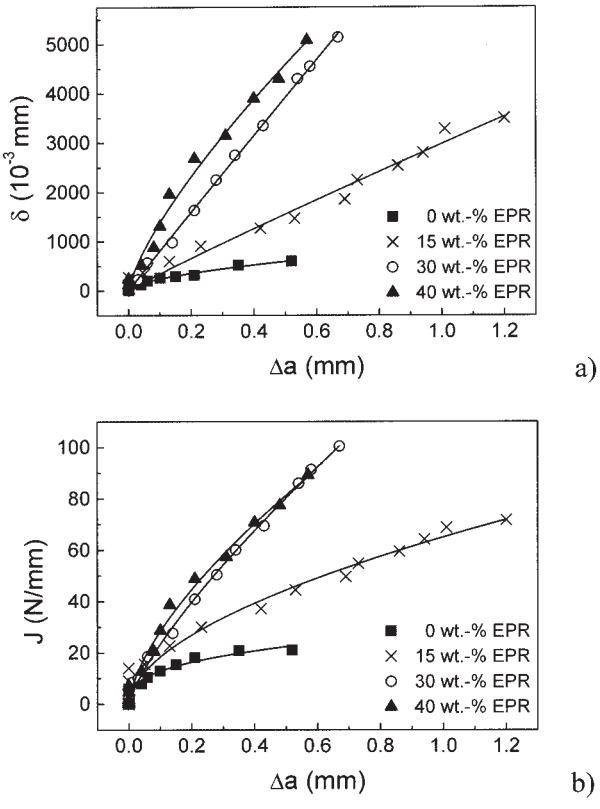

Figure 11 Crack-resistance curves from in situ investigations under quasi-static loadings: (a) δ_R curves and (b) J_R curves.

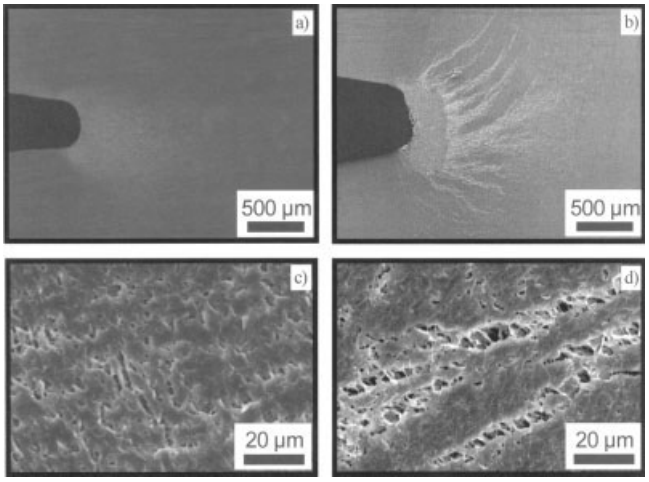

Figure 12 Crack-tip-deformation processes of a blend containing 50 wt % EPR: (a,c) impact loading and (b,d) quasi-static loading.

The δ value measured by in situ investigations contains the plastic, viscoelastic, and elastic deformations occurring at the crack tip. Therefore, the resistance against stable crack initiation measured by in situ investigations is much higher than the value determined by stretch zone measurements. In particular, the crack resistance rises in the region of small crack length with the EPR content.

The single-specimen method can be applied in an early stage of material development because only one specimen is necessary to register a complete crack-resistance curve. The material demand is much lower than that of the multiple-specimen method.

However, results of quasi-static in situ investigations cannot be compared with results of Charpy impact testing because of the time dependence of the polymer properties, including the toughness behavior.

Crack-tip-deformation behavior

The toughness behavior of polymer materials depends strongly on the kind of microdeformation process occurring near the crack tip, the energy that is dissipated thereby, and the range in which this process takes place. The dissipated energy to generate a single-craze respectively void is much lower than the energy that is dissipated during voiding associated with large plastic deformation of the matrix ligaments between the voids. The more the energy is dissipated, the higher the toughness is. In Figure 12, the microdeformations at the crack tip are shown for a blend containing 50 wt % EPR. At a dynamic loading, the deformation is voiding [Fig. 12(a,c)]. The deformed region in front of the crack tip is diffuse.

Under quasi-static loading conditions, the deformation mechanism is voiding associated with large plas-

tic deformation of the matrix ligaments [Fig. 12(b,d)]. δ is essentially larger because of the relaxation processes and plastic flow occurring at low testing speeds. Furthermore, the deformed region in front of the crack tip is much larger. Therefore, much more energy is dissipated, and the toughness values are much higher. The differences between deformed and undeformed regions in front of the crack tip can be recognized very well.

In both cases, a blunting of the crack tip can be observed. No stretch zone remains at the origin of the stable crack growth; the blunted crack tip grows through the specimen.

CONCLUSIONS

The instrumented Charpy impact test is the experimental basis for determining fracture mechanics values under impact loading conditions with respect to the temperature. The resistance of the material against stable crack initiation and propagation and against unstable crack propagation can be quantified. Both the energy-determined J value and the deformation-determined δ_d value show concurrent dependence on the EPR content for PP/EPR blends and on the temperature.

The transition from brittle material behavior to tough material behavior has been determined for each blend of the mixing series. Furthermore, the transition from tough material behavior to high-impact-toughness material behavior has been determined. A functional correlation between the EPR content and transition temperatures has been found. The EPR content decreases exponentially with increasing transition temperature. The determination of both transitions in correlation with morphological parameters can be used to determine application-oriented limits.

By the application of stability assessment diagrams, approximated instability values have been determined for a complete estimation of the dependence on material values as resistance against unstable crack propagation on the EPR content and temperature.

Crack-resistance curves can be achieved from results of the in situ measurements with only one specimen. This method is a suitable single-specimen method with a considerably lower material demand.

Crack-tip-deformation processes depend strongly on the loading rate. Voiding is a less energy-dissipating process than voiding associated with large plastic deformation of the matrix ligaments.

Fracture mechanics in conjunction with morphological analysis and methods of determination of microdeformation mechanisms contributes essentially to the field of application-oriented development of polymeric materials.[17]

References

1. Wu, S. Polymer 1985, 26, 1855.
2. Starke, J.-U.; Michler, G.; Grellmann, W.; Seidler, S.; Gahleitner, M.; Fiebig, J.; Nezbedova, E. Polymer 1998, 39, 75.
3. Borggreve, R. J. M.; Gaymans, R. J.; Schuijer, J.; Ingen Housz, J. F. Polymer 1987, 28, 1489.
4. Margolina, A. Polym Commun 1990, 31, 95.
5. Mamat, A.; Vu-Khanh, T.; Cigana, P.; Favis, B. D. J Polym Sci Part B: Polym Phys 1997, 35, 2583.
6. Grellmann, W.; Seidler, S.; Jung, K.; Kotter, I. J Appl Polym Sci 2001, 79, 2317.
7. Plastics—Determination of Charpy Impact Properties, Part 2: Instrumented Impact Test; ISO 179-2; International Organization for Standardization: Geneva, Switzerland, 1997.
8. Deformation and Fracture Behaviour of Polymers; Grellmann, W.; Seidler, S., Eds.; Springer-Verlag: New York, 2001.
9. Han, Y.; Lach, R.; Grellmann, W. J Appl Polym Sci 2000, 75, 1605.
10. Sumpter, J. D.; Turner, C. E. Int J Fracture 1973, 9, 320.
11. Paris, P. C.; Jonson, R. E. ASTM STP 1983, 803(II), 5.
12. Plastics—Determination of Tensile Properties; ISO 527; International Organization for Standardization: Geneva, Switzerland, 1993.
13. Plastics—Determination of Flexural Properties; ISO 178; International Organization for Standardization: Geneva, Switzerland, 2001.
14. Plastics—Determination of Charpy Impact Properties, Part 1: Non-Instrumented Impact Test; ISO 179-1; International Organization for Standardization: Geneva, Switzerland, 2000.
15. Han, Y.; Lach, R.; Grellmann, W. J Appl Polym Sci 2001, 79, 9.
16. Seidler, S.; Koch, T.; Kotter, I.; Grellmann, W. Proceedings of Euromat 2000; Elsevier Science: Amsterdam, 2000; Chapter 1, p 255.
17. Kotter, I. Morphologie-Zähigkeits-Korrelationen von EPR-modifizierten Polypropylenwerkstoffen; Mensch & Buch: Berlin, 2003.